

# NONPARAMETRIC ESTIMATION AND BOOTSTRAP INFERENCE ON TRENDS IN ATMOSPHERIC TIME SERIES: AN APPLICATION TO ETHANE<sup>\*</sup>

Marina Friedrich<sup>a,b</sup>, Eric Beutner<sup>a</sup>, Hanno Reuvers<sup>c</sup>, Stephan Smeekes<sup>a</sup>, Jean-Pierre Urbain<sup>†a</sup>, Whitney Bader<sup>d</sup>, Bruno Franco<sup>e</sup>, Bernard Lejeune<sup>d</sup>, and Emmanuel Mahieu<sup>d</sup>

<sup>a</sup>Maastricht University - Department of Quantitative Economics

<sup>b</sup>Potsdam Institute for Climate Impact Research - Member of the Leibniz Association

<sup>c</sup>Erasmus University Rotterdam

<sup>d</sup>University of Liège - Institute of Astrophysics and Geophysics

<sup>e</sup>Université libre de Bruxelles (ULB) - Service de Chimie Quantique et Photophysique

## Abstract

Understanding the development of trends and identifying trend reversals in decadal time series is becoming more and more important. Many climatological and atmospheric time series are characterized by autocorrelation, heteroskedasticity and seasonal effects. Additionally, missing observations due to instrument failure or unfavorable measurement conditions are common in such series. This is why it is crucial to apply methods which work reliably under these circumstances. The goal of this paper is to provide a toolbox which can be used to determine the presence and form of changes in trend functions using parametric as well as nonparametric techniques.<sup>1</sup> We consider bootstrap inference on broken linear trends and smoothly varying nonlinear trends. In particular, for the broken trend model, we propose a bootstrap method for inference on the break location and the corresponding changes in slope. For the smooth trend model we construct simultaneous confidence bands around the nonparametrically estimated trend. Our autoregressive wild bootstrap approach combined with a seasonal filter, is able to handle all issues mentioned above. We apply our methods to a set of atmospheric ethane series with a focus on the measurements obtained above the Jungfraujoch in the Swiss Alps. Ethane is the most abundant non-methane hydrocarbon in the Earth's atmosphere, an important precursor of tropospheric ozone and a good indicator of oil and gas production as well as transport. Its monitoring is therefore crucial for the characterization of air quality and of the transport of tropospheric pollution.

---

<sup>\*</sup>Corresponding author: Marina Friedrich, E-mail: [friedrich@pik-potsdam.de](mailto:friedrich@pik-potsdam.de), Tel: +49-331-288-20799. Support to the Liège team has been primarily provided by the F.R.S. - FNRS (Brussels) under Grant J.0147.18. Emmanuel Mahieu is a Research Associate with F.R.S. - FNRS. The vital support from the GAW-CH programme of MeteoSwiss is acknowledged. Mission expenses at the Jungfraujoch station were funded by the Fédération Wallonie-Bruxelles. We thank the International Foundation High Altitude Research Stations Jungfraujoch and Gornergrat (HFSJG, Bern) for supporting the facilities needed to perform the observations. W. Bader has received funding from the European Union's Horizon 2020 research and innovation programme under the Marie Skłodowska-Curie grant agreement no. 704951, and from the University of Toronto through a Faculty of Arts & Science Postdoctoral Fellowship Award.

<sup>†</sup>Deceased on October 1, 2016

<sup>1</sup>We provide R code for all proposed methods on <https://www.pik-potsdam.de/members/marinafr>.

# 1 Introduction

In the presence of global climate change, understanding the development of decadal time series becomes more and more relevant. A major part of this understanding lies in the analysis of time trends and the detection of trend reversals. Many tools are available for this purpose in the econometrics and statistics literature. They range from linear trend analysis to more advanced methods such as trends with breaks, polynomial trends, or smooth trends of unspecified form. Estimation of the trend, however, is not enough; it is crucial that with every estimate we can indicate the corresponding uncertainty around it. This is commonly achieved by calculating confidence intervals which enable us to judge the significance of our results.

Climatological data, however, frequently display characteristics which complicate the calculation of such uncertainty measures. These characteristics can include strong seasonality, different degrees of variability in the data, such as significant inter-annual changes, and missing observations due to instrument failures or unfavorable measurement conditions. Therefore, it is important to use methods which provide reliable results even under these circumstances. A prominent example in which the three problematic characteristics arise is atmospheric ethane, when measured with the ground-based Fourier Transform InfraRed (FTIR) technique. It displays strong seasonality, a time-varying variance and, since measurements can only be taken under clear sky conditions, has many missing data points.

It is increasingly popular to resort to bootstrap methods to address these problems. Similar arguments are presented in Gardiner et al. (2008) who propose a method for trend analysis of greenhouse gases. Their approach estimates a linear trend using least squares minimization. Subsequently, to obtain confidence intervals for the slope parameter, they introduce an i.i.d. (independently and identically distributed) bootstrap method.

This combination of linear trend estimation and i.i.d. bootstrap has been applied to investigate trends in various data series; see e.g. De Smedt et al. (2010), Mahieu et al. (2014), Franco et al. (2015) and Hausmann et al. (2016). The latter paper uses the bootstrap method to study trends in atmospheric methane and ethane concentrations measured at Zugspitze and Lauder. They split the sample into two time periods and compare the changes in trends between both periods.

This approach, however, suffers from two major drawbacks. First, in the presence of autocorrelation, the i.i.d. bootstrap method cannot correctly mimic the dependence structure of the residuals. Alternative bootstrap methods are available which can solve this problem and they require just minor modifications in implementation. Second, the approach does not provide a formal test if and where the sample should be split and it does not give a measure of uncertainty regarding the location of the obtained break.

The aim of this paper is to propose a toolbox for trend estimation which addresses these drawbacks. We give an overview of selected statistical and econometric tools designed for the analysis of time trends and trend reversals. We focus on two different, but complimentary approaches which are particularly suited in this context. In the first part, we present a linear trend model which allows for a break at an unknown time point. It provides researchers with a tool to test if there was a break present in the trend and, if so, it additionally gives an estimate of its location with a

reliable confidence interval.

In the second part, we move to a more general specification by considering a smoothly varying trend model. This approach is more flexible as it does not impose any assumptions regarding the form of the trend. We propose three additional methods in which we take a closer look at the trend obtained from this approach. First, we identify the locations of (local) extrema, as they are typically associated with trend reversal, and propose a method to construct a confidence interval around the locations. Second, we investigate a method for testing if the trend can be described by a specific parametric form. We test if the trend (possibly in a subsample) can adequately be described by a parametric function, such as a linear one. Third, we provide a test for monotonicity of the trend function on a subsample, which does not require fitting a parametric function, but can directly be applied on the nonparametrically estimated trend.

In both parts, we suggest the use of bootstrap methods. They can be used for the construction of confidence intervals as well as to obtain critical values for the tests. We advocate the use of a specific bootstrap method – the autoregressive wild bootstrap – which is applicable to correlated data. Its second advantage over many other bootstrap methods is that it can easily be applied to data series with missing observations.

All methods are used to study the atmospheric ethane ( $\text{C}_2\text{H}_6$ ) burden with the help of a set of six time series. The series consist of daily ethane columns (i.e. the number of molecules integrated between the ground and the top of the atmosphere in a column of a given area, e.g. a square centimeter) obtained from ground-based FTIR measurements. In particular, we will focus on the Jungfraujoch ethane measurements.

The structure of the paper is as follows. In Section 2, we present the data. Section 3 introduces the linear trend approach. We show how to determine the break point, how to estimate the trend and how to construct confidence intervals. Section 4 continues with the nonparametric trend model, its estimation and confidence intervals. In this section, we also present how to conduct inference on the shape of the nonparametric trends. At the end of each section, the respective methods are applied to the data. Section 5 concludes.

## 2 The ethane data

Ethane is the most abundant non-methane hydrocarbon in the Earth’s atmosphere and has several properties which make it important to study. First, ethane is an indirect greenhouse gas influencing the atmospheric lifetime of methane. It degrades by reacting with the same oxidizer which is needed for the degradation of other major greenhouse gases like e.g. methane. Molecules of the oxidizer which are occupied by ethane are not available for the destruction of other pollutants. Second, ethane is an important precursor of tropospheric ozone. It contributes to the formation of ground level ozone ( $\text{O}_3$ ) which is a major pollutant affecting the air quality. While ozone in higher levels of the atmosphere protects us from the Sun’s harmful ultraviolet rays, ground level ozone damages ecosystems and has adverse effects on the human body. Third, ethane emissions can be used as a measure of methane emissions. Both gases are co-emitted from the oil and gas exploitation, while ethane does not have significant natural sources, methane is released in the atmosphere by both

natural activities and human-induced ones. This makes it hard to measure the fraction of methane released by the oil and gas sector. An estimate of this fraction can be provided with the help of ethane measurements. Its monitoring is therefore crucial for the characterization of air quality and of the transport of tropospheric pollution. The main sources of ethane are located in the Northern hemisphere, and the dominating emissions are associated with production and transport of oil and natural gas.

We illustrate our proposed methods by analyzing time trends in six series of atmospheric ethane measurements. In the text we focus, however, on one series which is derived from observations performed at the Jungfrauoch station in the Swiss Alps. It is located on the saddle between the Jungfrau and the Mönch, located at  $46.55^\circ$  N,  $7.98^\circ$  E, 3580 m altitude. Results obtained from the other five data series will be summarized in tables and related graphs can be found in the Appendix.

The Jungfrauoch ethane series has been studied in detail in Franco et al. (2015). The paper also provides further details on the ground-based station at Jungfrauoch and on how the measurements are obtained. We focus on this series, because measurement conditions are very favorable at this location due to high dryness and low local pollution. It is a time series consisting of daily ethane columns recorded under clear-sky conditions between September 1994 and August 2014 with a total of 2260 data points. For the location and sample size of the other five series we refer to the first column of Table 1 in the next section.

Giving an indication of the severity of the missing data problem present in this series, the Jungfrauoch series contains an average number of data points per year of 112.6. The situation is similar in the other series. In addition to missing data points, the series also exhibit seasonality. Ethane degrades faster under warm weather conditions than in cold temperature and therefore, the measurements display local peaks every winter period.

All results in the following sections are obtained using  $B = 999$  replications of the bootstrap procedure. Whenever confidence intervals or bands are given, these are for a nominal coverage level of 95%.

### 3 The linear trend approach

We consider a linear trend model including the possibility of a break in the trend line. At the breakpoint, the slope of the trend function is allowed to change. The intercept change is restricted in such a way that there will be no discontinuity at the break, i.e. no jump between the consecutive linear functions. In this section, we first present the model specifications. Second, we show how the model can be estimated. Third, the bootstrap method for the construction of confidence intervals is introduced. The final part applies the proposed approach to the data.

#### 3.1 A broken trend model

We consider a linear regression with the following specification. For  $t = 1, \dots, T$ ,

$$y_t = \alpha + \beta t + \delta D_{t,T_1} + F_t + u_t, \tag{3.1}$$

where

$$D_{t,T_1} = \begin{cases} 0 & \text{if } t \leq T_1, \\ t - T_1 & \text{if } t > T_1. \end{cases} \quad (3.2)$$

In this specification,  $\{y_t\}$  is the time series of interest,  $t$  refers to the time trend with slope parameter  $\beta$  and  $\alpha$  is the intercept. The break occurs at time  $T_1$ . The variable  $D_{t,T_1}$  is a dummy variable which induces a change in the slope coefficient from  $\beta$  to  $(\beta + \delta)$  after  $T_1$ . At the same time, the intercept of the trend function changes in such a way that the successive linear components are joined at the breakpoint. Additionally, the term  $F_t$  captures the intra-annual variability, which is present in almost all climate time series, with the help of Fourier terms

$$F_t = \sum_{j=1}^M a_j \cos(2j\pi t) + b_j \sin(2j\pi t). \quad (3.3)$$

This specification of the seasonal variability is widely used when estimating trends in atmospheric gases, see e.g. Gardiner et al. (2008), Franco et al. (2015) and Franco et al. (2016). It has been shown in these papers that the variability is well captured by the inclusion of three sine and cosine terms. We follow the same approach and will consider equation (3.3) with  $M = 3$  in the remainder of the paper. The errors  $\{u_t\}$  are allowed to be serially correlated and to exhibit changes in variance. The goal is to estimate  $(\alpha, \beta, \delta)$ . The parameters of equation (3.3) will also be estimated during the process and we will denote the fitted version by  $\hat{F}_t$ . To formalize the above mentioned missing data problem, we note that we observe a part of the observations  $y_1, \dots, y_T$ . We define a binary variable  $M_t$  as

$$M_t = \begin{cases} 1 & \text{if } y_t \text{ is observed} \\ 0 & \text{if } y_t \text{ is missing} \end{cases} \quad t = 1, \dots, T. \quad (3.4)$$

We assume that the missing pattern, characterized by  $\{M_t\}$ , is independent of the observations and can be weakly dependent with the dependence decaying to zero over time. It is reasonable to assume that the pattern of the missing data points in the case of FTIR measurements follows these assumptions. A more detailed discussion on this issue can be found in Friedrich et al. (2019).

Before we continue with a description of the estimation procedure, we give a formal test to determine whether a model with one break is preferred over a simple linear trend model. It is based on Bai and Perron (1998). Let  $\Lambda = [\lambda T, (1 - \lambda)T]$ , with  $0 < \lambda < 1/2$ . By using  $\Lambda$  as a set for possible break dates, we ensure that a candidate break,  $T_c$ , is neither too close to the beginning of the sample nor too close to the end. Otherwise, the number of observations on each side of the candidate break would not be sufficient for further estimation. We use the test statistic

$$S_T = \min_{\alpha, \beta, F_t} \sum_{t=1}^T M_t (y_t - \alpha - \beta t - F_t)^2 - \inf_{T_c \in \Lambda} \min_{\alpha, \beta, \delta, F_t} \sum_{t=1}^T M_t (y_t - \alpha - \beta t - \delta D_{t,T_c} - F_t)^2, \quad (3.5)$$

where we compare the sum of squared residuals of a model without break to the lowest sum of

squared residuals of a model including one break. It is a formal test of the pair of hypothesis  $H_0 : \delta = 0$  versus  $H_1 : \delta \neq 0$ , for every possible break point  $T_c$ . For high values of  $S_T$ , there is evidence that the model with break fits the data better and we reject  $H_0$ ; for low values we fail to reject it. Given a significance level of the test, the critical value of the test determines the cut-off point and we obtain it using the autoregressive wild bootstrap. Further details on this bootstrap method are postponed to Section 3.3.

### 3.2 Estimation

The first step in the procedure is to estimate the break date. Subsequently, given the estimated break date, the parameter estimates of interest are determined. Given a candidate break date  $T_c$ , estimates of  $(\alpha, \beta, \delta, F_t)$  are obtained by minimizing the following sum of squared residuals

$$\left(\hat{\alpha}_{T_c}, \hat{\beta}_{T_c}, \hat{\delta}_{T_c}, \hat{F}_{t,T_c}\right) = \underset{\alpha, \beta, \delta, F_t}{\operatorname{argmin}} \sum_{t=1}^T M_t (y_t - \alpha - \beta t - \delta D_{t,T_c} - F_t)^2, \quad (3.6)$$

where we make explicit that these estimates are for a candidate break date and not the final parameter estimates by using a subscript  $T_c$ . Let us come back to the two step procedure. For the first step, which is estimating the break location, we need to construct such a sum of squared residuals for every admissible break date candidate  $T_c$ . The minimum over all possible candidates gives us the estimated break date. Let  $\Lambda$  be the same set as in the previous section and consider the following minimization problem

$$\hat{T}_1 = \underset{T_c \in \Lambda}{\operatorname{argmin}} \sum_{t=1}^T M_t \left(y_t - \hat{\alpha}_{T_c} - \hat{\beta}_{T_c} t - \hat{\delta}_{T_c} D_{t,T_c} - \hat{F}_{t,T_c}\right)^2, \quad (3.7)$$

where  $(\hat{\alpha}_{T_c}, \hat{\beta}_{T_c}, \hat{\delta}_{T_c}, \hat{F}_{t,T_c})$  are determined as described above. Once we have obtained the estimate of the break date,  $\hat{T}_1$ , we construct the corresponding least-squares parameter estimates in the second step. To be consistent with the notation, these will be denoted as  $(\hat{\alpha}, \hat{\beta}, \hat{\delta}, \hat{F}_t) = (\hat{\alpha}_{\hat{T}_1}, \hat{\beta}_{\hat{T}_1}, \hat{\delta}_{\hat{T}_1}, \hat{F}_{t,\hat{T}_1})$ .

### 3.3 Confidence intervals

Given the parameter estimates and the estimated break location, we need to rely on a measure of uncertainty to be able to judge the significance of our findings. A major difficulty with climate time series is the presence of serial correlation of the residuals from our estimated model. An additional complication arises due to the fact that these time series are mostly made of observations which are unequally spaced over the sample period  $t = 1, \dots, T$ . To overcome these difficulties, we propose a bootstrap method which has been established in the econometrics and statistics literature as being very successful and providing accurate confidence intervals even in small samples. It solves both, the problem caused by serial correlation and the unequally spaced data. In addition, it protects against possible changes in variance of the residuals.

To form bootstrap samples, the standard bootstrap method – the i.i.d. bootstrap – draws

randomly and with replacement from the residuals and, thereby, destroys both the dependence structure and possible time variations in the variance. Due to these reasons, the bootstrap sample will not correctly reflect the original series of residuals and the general principle, on which bootstrap methods are based, is violated. The goal, therefore, is to construct bootstrap errors which have the same pattern of correlation, variance changes and missing data as the original set of residuals. The autoregressive wild bootstrap, which is proposed in the context of nonparametric trend estimation in Friedrich et al. (2019), is to our knowledge the best way to achieve this goal. In particular, in the presence of serial correlation compared to its competitors – sieve or block bootstrap methods – it holds a clear advantage as it has a natural way of handling missing data. No adjustments are needed for it to reproduce the missing data pattern in the original sample.

In the remainder of this section, we present details on this bootstrap method by giving the bootstrap algorithm for the case of the break location. We then explain how it can easily be adapted to form confidence intervals for the parameter estimates of slope and intercept. To determine confidence intervals for the break date estimate, we use the following bootstrap algorithm:

**Algorithm 1** (Autoregressive Wild Bootstrap - Break location).

1. Calculate residuals from the estimation of Model (3.1). Impose a break at  $\hat{T}_1$ . For  $t = 1, \dots, T$ ,

$$\hat{u}_t = M_t \left( y_t - \hat{\alpha} - \hat{\beta}t - \hat{\delta}D_{t,\hat{T}_1} - \hat{F}_t \right).$$

2. For  $0 < \gamma < 1$ , generate  $\nu_1^*, \dots, \nu_n^*$  as i.i.d.  $\mathcal{N}(0, 1 - \gamma^2)$  and let  $\xi_t^* = \gamma\xi_{t-1}^* + \nu_t^*$  for  $t = 2, \dots, T$ . Take  $\xi_1^* \sim \mathcal{N}(0, 1)$  to ensure stationarity of  $\{\xi_t^*\}$ .
3. Calculate the bootstrap errors  $u_t^* = M_t \xi_t^* \hat{u}_t$  and create the bootstrap sample as

$$y_t^* = M_t \left( \hat{\alpha} + \hat{\beta}t + \hat{\delta}D_{t,\hat{T}_1} + \hat{F}_t + u_t^* \right)$$

for  $t = 1, \dots, T$ , using the same estimated coefficients as in Step 1.

4. Determine  $\hat{T}_1^*$  from  $y_t^*$  as in (3.7) and store the estimates.
5. Repeat Steps 2 to 4  $B$  times to obtain the bootstrap distribution of  $\hat{T}_1^*$ .

Note that in Step 2 we generate  $\{\xi_t^*\}$  for all  $t = 1, \dots, T$ , although in Step 3 we construct bootstrap errors and subsequently, bootstrap observations only when there exists an actual data point. This is what the multiplication by  $M_t$  in Step 3 ensures. The bootstrap sample thus correctly reflects the missing pattern present in the data.

In Step 2 of the above algorithm, the autoregressive coefficient  $\gamma$  has to be chosen. To obtain an asymptotically valid bootstrap method, that is, bootstrap confidence intervals whose confidence level approaches  $(1 - \alpha)$  in the limit, Friedrich et al. (2019) show that  $\gamma$  should tend to 1 as the sample size  $T$  increases. Friedrich et al. (2019) suggest to achieve this by setting  $\gamma = \theta^{1/l}$  with  $l = 1.75T^{1/3}$  and  $\theta = 0.1$ .

The confidence intervals are then determined by the  $\alpha/2$  quantile and  $(1 - \alpha/2)$  quantile of the bootstrap distribution. In analogy to this algorithm, we can obtain confidence intervals for the

parameter estimates by adjusting Step 4. Given the estimated break location  $\hat{T}_1$ , we estimate Model (3.1) from  $y_t^*$ , thereby imposing the same break as found in the data. The bootstrap estimates  $\hat{\alpha}^*$ ,  $\hat{\beta}^*$  and  $\hat{\delta}^*$  are stored and the corresponding bootstrap distributions and quantiles are constructed in the same way as in the previously described case.

The same bootstrap method is also used to obtain critical values for the test statistic  $S_T$  as in (3.5). The approach is very similar to above. In this application, however, the bootstrap series are constructed under the null hypothesis of no break, meaning that a linear trend model without break is estimated from the data in Step 1 and then used to form residuals. Once the bootstrap series is constructed using the linear trend from Step 1, the bootstrap version of the test statistic  $S_T^*$  is determined.

**Algorithm 2** (Autoregressive Wild Bootstrap - Break test).

1. Calculate residuals from the estimation of Model (3.1) with  $\delta = 0$ . For  $t = 1, \dots, T$ ,

$$\hat{u}_t = M_t \left( y_t - \hat{\alpha} - \hat{\beta}t - \hat{F}_t \right).$$

2. Identical to Step 2 of Algorithm 1.

3. Calculate the bootstrap errors  $u_t^* = M_t \xi_t^* \hat{u}_t$  and create the bootstrap sample as

$$y_t^* = M_t \left( \hat{\alpha} + \hat{\beta}t + \hat{F}_t + u_t^* \right)$$

for  $t = 1, \dots, T$ , using the same estimated coefficients as in Step 1.

4. Obtain  $S_T^*$  from  $y_t^*$  as in equation (3.5) and store the result.

5. Repeat Steps 2 to 4  $B$  times to obtain the bootstrap distribution of  $S_T^*$ .

Since the test is rejected for large values of the test statistic  $S_T$ , we use the  $(1 - \alpha)$  quantile of the ordered bootstrap statistics as critical value for the break test.

### 3.4 Data application

We now present results of an application of the tools to the ethane time series. The statistical tests which help us to decide whether a break is present in the trend line give strong evidence for the alternative hypothesis in all series, thus indicating that a model with a break should be preferred over a simple linear trend model. Detailed results of the tests for all six time series are summarized in Table 1.

We find a breakpoint in the Jungfraujoch ethane column series in the beginning of 2009. This is in line with the findings of Franco et al. (2015). In addition to the point estimate of the break location, which is 2009.21, the autoregressive wild bootstrap enables us to find a confidence interval for this break ranging from 2008.35 to 2010.03. The results are summarized graphically in Figure 1 which plots the ethane time series (gray circles), the seasonal fit of three Fourier terms (blue) as well as the estimated broken trend (black). The confidence interval for the break location is indicated



	$T$	$p$ -value	$\mathcal{F}_T$	$CV$	<i>Discussed in</i>
Jungfraujoch	2260	0.0000	$6.22 \times 10^{32}$	$0.52 \times 10^{32}$	Franco et al. (2015)
Boulder	164	0.0225	$1.71 \times 10^{32}$	$1.27 \times 10^{32}$	Franco et al. (2016)
Eureka	725	0.0049	$8.79 \times 10^{31}$	$5.16 \times 10^{31}$	Franco et al. (2016)
Lauder	2550	0.0248	$2.82 \times 10^{31}$	$2.30 \times 10^{31}$	Zeng et al. (2012)
Thule	814	0.0000	$1.99 \times 10^{32}$	$0.75 \times 10^{32}$	Franco et al. (2016)
Toronto	1399	0.0000	$1.93 \times 10^{33}$	$2.84 \times 10^{32}$	Franco et al. (2016)

Table 1: Results of the break tests ( $\pi = 0.1$ )

by the two dotted vertical lines. Before the break, there is a significant downward trend, which turns into an upward trend after the break. The slope after the break is positive. The estimates are presented in Table 2 for all six series. In addition, Figure 4 in the Appendix plots these results in the same fashion as in Figure 1.

As mentioned by Franco et al. (2015), the initial downward trend can be explained by a general emission reduction since the mid 1980's, of the fossil fuel sources in the Northern Hemisphere. The upward trend seems to be a more recent phenomenon. There are studies that attribute it to the recent growth in the exploitation of shale gas and tight oil reservoirs, taking place in North America, see e.g. Vinciguerra (2015), Franco et al. (2016) and Helmig et al. (2016). The significant negative coefficients before and after the break in Table 2 indicate that Lauder is not yet impacted

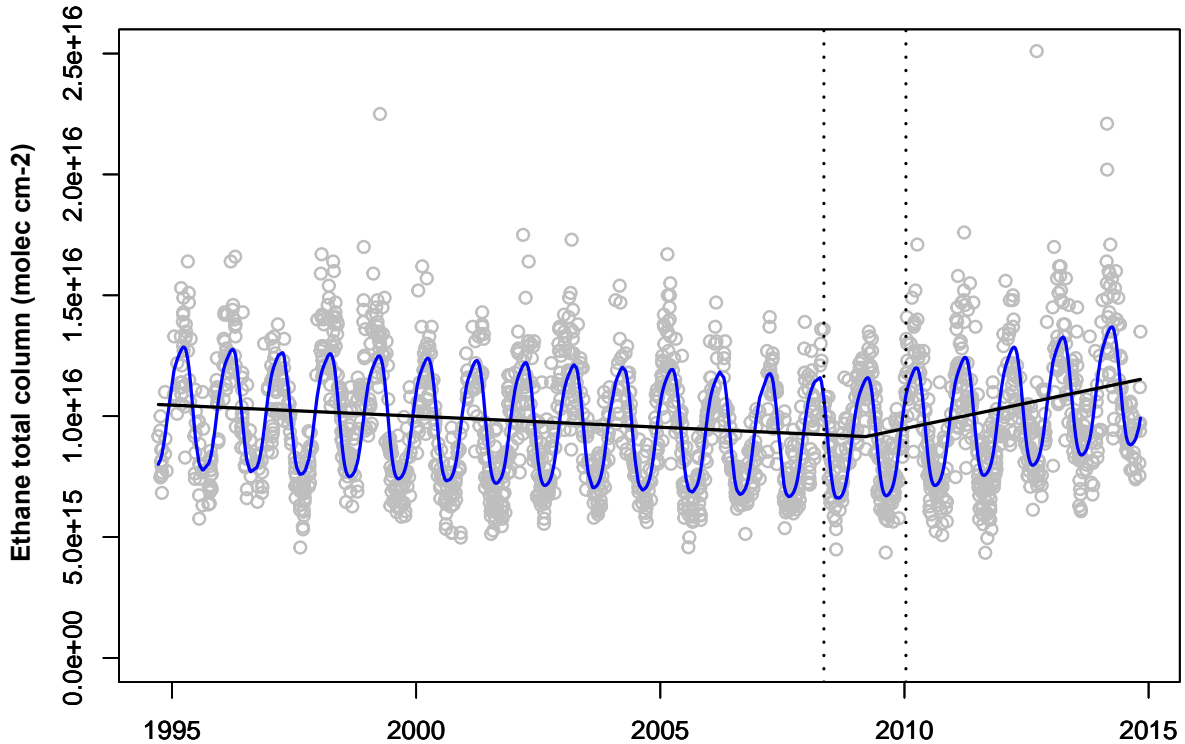


Figure 1: Breakpoint estimate and confidence interval for Jungfraujoch

	break date [CI]	<i>period</i>	slope estimate [CI]
Jungfraujoch	2009.21 [2008.35,2010.03]	<i>before</i>	$-9.15 \times 10^{13}$ [ $-1.14 \times 10^{14}, -6.94 \times 10^{13}$ ]
		<i>after</i>	$4.21 \times 10^{14}$ [ $3.44 \times 10^{14}, 4.99 \times 10^{14}$ ]
Boulder	2014.48 [2014.01,2014.48]	<i>before</i>	$9.37 \times 10^{14}$ [ $4.20 \times 10^{14}, 1.46 \times 10^{15}$ ]
		<i>after</i>	$-4.48 \times 10^{16}$ [ $-6.56 \times 10^{16}, -2.40 \times 10^{16}$ ]
Eureka	2010.15 [2008.64,2014.15]	<i>before</i>	$-1.78 \times 10^{13}$ [ $-1.91 \times 10^{14}, 1.55 \times 10^{14}$ ]
		<i>after</i>	$5.78 \times 10^{14}$ [ $3.98 \times 10^{14}, 7.60 \times 10^{14}$ ]
Lauder	2001.35 [1995.66,2010.81]	<i>before</i>	$-1.62 \times 10^{14}$ [ $-1.97 \times 10^{14}, -1.26 \times 10^{14}$ ]
		<i>after</i>	$-9.06 \times 10^{13}$ [ $-1.08 \times 10^{14}, -7.26 \times 10^{13}$ ]
Thule	2007.32 [2003.71,2011.18]	<i>before</i>	$-2.19 \times 10^{14}$ [ $-3.51 \times 10^{14}, -8.68 \times 10^{13}$ ]
		<i>after</i>	$3.00 \times 10^{14}$ [ $1.89 \times 10^{14}, 4.14 \times 10^{14}$ ]
Toronto	2009.01 [2008.06,2010.04]	<i>before</i>	$-2.96 \times 10^{14}$ [ $-4.51 \times 10^{14}, -1.40 \times 10^{14}$ ]
		<i>after</i>	$1.04 \times 10^{15}$ [ $8.64 \times 10^{14}, 1.20 \times 10^{15}$ ]

Table 2: Point and interval estimates of slope parameter  $\beta$

by the recent increase of ethane in the Northern hemisphere, further from the main emission sources. Lauder is the only site in the data set which is located in the Southern hemisphere. Indeed, ethane has a mean atmospheric lifetime of 2 months, significantly shorter than the time needed to mix air between both hemispheres.

## 4 A smooth trend function

While the previous analysis restricted the trend to a (broken) linear form, in this section, we look at an alternative trend model. It is more flexible in the sense that it does not require us to specify a specific form of the trend in advance. This section is divided into two main parts. The first part follows the structure of the previous section. In the second part, we propose several tests which allow us to further investigate the obtained results.

### 4.1 The nonparametric trend model

As an alternative model specification, we look at the following nonparametric trend model

$$y_t = g(t/T) + F_t + u_t \quad t = 1, \dots, T, \quad (4.1)$$

where  $F_t$  is the same series of Fourier terms as in equation (3.3). As above, we only observe a part of the data. We allow for heteroskedasticity and additionally, serial correlation is captured by allowing  $\{u_t\}$  to be weakly dependent over time with the dependence dying out. For details on the explicit assumptions we refer to Friedrich et al. (2019). The nonparametric trend specification has the advantage that no particular form of the trend function has to be imposed. While in the previous section, we assume that the data are following Model (3.1) - a linear trend with one break - we are

more flexible regarding the trend function in this case. The function  $g(\cdot)$  can be of any form as long as it is smooth in the sense that it is twice continuously differentiable with bounded derivatives. Estimation is done using a two-stage procedure to first eliminate the seasonal variability and then estimate the trend function nonparametrically. Inference on the estimated trend is conducted using the autoregressive wild bootstrap to construct pointwise intervals in a similar fashion as above. Subsequently, we apply a simple three step algorithm to find simultaneous confidence bands based on the pointwise intervals. Details are given in the next two subsections.

#### 4.1.1 Estimation

The main goal is to estimate the trend function  $g(\cdot)$  and to determine the uncertainty around this estimate. To achieve this goal we propose a two-stage estimation procedure. In the first stage,  $y_t$  is regressed on the Fourier terms and in the second stage, the residuals from the first stage are used to estimate the trend nonparametrically. Denote by  $\hat{u}_t$  the residuals from a regression of  $y_t$  on the Fourier terms so that  $\hat{u}_t = M_t(y_t - \hat{F}_t)$ . To estimate the trend function from  $\{\hat{u}_t\}$ , we apply a nonparametric kernel estimator: the local constant Nadaraya-Watson estimator. It is found by minimizing a weighted sum of squares with respect to  $g(\cdot)$ . This is done for every point  $t = 1, \dots, T$ . As is standard with this approach, we map the points into the interval  $(0, 1)$ . Thus, for  $\tau \in (0, 1)$ , we obtain:

$$\begin{aligned} \hat{g}(\tau) &= \arg \min_{g(\tau)} \sum_{t=1}^T K\left(\frac{t/T - \tau}{h}\right) M_t \{\hat{u}_t - g(\tau)\}^2 \\ &= \left[ \sum_{t=1}^T K\left(\frac{t/T - \tau}{h}\right) M_t \right]^{-1} \sum_{t=1}^T K\left(\frac{t/T - \tau}{h}\right) M_t \hat{u}_t, \end{aligned} \quad (4.2)$$

where  $K(\cdot)$  is a kernel function and  $h > 0$  is the bandwidth. We propose to use the Epanechnikov kernel given by  $K(x) = \frac{3}{4}(1 - x^2)\mathbb{1}_{\{|x| \leq 1\}}$ . The parameter  $h$  is a smoothing parameter. Large bandwidths produce a very smooth estimate, while for small bandwidth, the trend becomes less smooth. Bandwidth selection is an important aspect for this type of estimation. Therefore, we propose using a data-driven selection method valid for time series applications, called modified cross-validation (MCV). It is based on the original criterion proposed in Chu and Marron (1991):

$$CV_k(h) = \frac{1}{T} \sum_{t=1}^T M_t \left( \hat{g}_{k,h}\left(\frac{t}{T}\right) - \hat{u}_t \right)^2 \quad (4.3)$$

where

$$\hat{g}_{k,h}(t/T) = \frac{(T - 2k - 1)^{-1} \sum_{t:|t-\tau T|>k} K\left(\frac{t/T-\tau}{h}\right) M_t \hat{u}_t}{(T - 2k - 1)^{-1} \sum_{t:|t-\tau T|>k} K\left(\frac{t/T-\tau}{h}\right) M_t} \quad (4.4)$$

leaves out the  $(2k + 1)$  observations receiving the highest weight. The optimal bandwidth is found by minimizing this criterion with respect to  $h$ . We elaborate on the practical implementation and give an example during the application in Section 4.1.3.

### 4.1.2 Confidence intervals

As we argued above, to merely rely on point estimates of the trend function to draw conclusions about the underlying trend is not sufficient. Confidence intervals are needed to say more about the significance of the trend. In this setting, the object of interest is the trend function as a whole and there is no single parameter which summarizes certain features of this function – like the slope coefficient in the previous approach. Therefore, it is crucial to have a tool to judge the significance over more than one time point, preferably, over the whole sample. Confidence intervals which allow for this could be used, for example, to assess whether there has been a significant non-zero upward or downward trend. This could be checked by trying to place a straight line as a trend function and then observing if this line can be completely embedded within the confidence intervals.

Confidence bands, where the coverage simultaneously holds over more than one point or even the whole sample can be constructed from pointwise confidence intervals. We therefore first propose a method to construct pointwise confidence intervals for the nonparametric trend estimate. Second, we suggest a three-step algorithm to transform pointwise intervals into simultaneous confidence bands. For this type of model, it has been shown in the statistical literature that bootstrap methods are a reliable tool to conduct inference (see e.g. Bühlmann (1998), Neumann and Polzehl (1998)). We again propose to use the autoregressive wild bootstrap. A minor adjustment compared to the above algorithm has to be made. Therefore, we give the full bootstrap algorithm again, for completeness.

**Algorithm 3** (Autoregressive Wild Bootstrap - Nonparametric trend).

1. Let  $\tilde{g}(\cdot)$  be defined as in (4.2), but using bandwidth  $\tilde{h}$ . Obtain residuals

$$\hat{\epsilon}_t = M_t(\hat{u}_t - \tilde{g}(t/T)), \quad t = 1, \dots, T.$$

2. Identical to Step 2 of Algorithms 1 and 2.
3. Calculate the bootstrap errors  $\epsilon_t^*$  as  $\epsilon_t^* = M_t \xi_t^* \hat{\epsilon}_t$  and generate the bootstrap observations by

$$\hat{u}_t^* = M_t(\tilde{g}(t/T) + \epsilon_t^*), \quad t = 1, \dots, n,$$

where  $\tilde{g}(t/T)$  is the same estimate as in the first step.

4. Obtain the bootstrap estimator  $\hat{g}^*(\cdot)$  as defined in (4.2) using the bootstrap series  $\hat{u}_t^*$ , with the same bandwidth  $h$  as used for the original estimate  $\hat{g}(\cdot)$ .
5. Repeat Steps 2 to 4 a total of  $B$  times and let

$$\hat{q}_\alpha(\tau) = \inf \{u; P^* [\hat{g}^*(\tau) - \tilde{g}(\tau) \leq u] \geq \alpha\}$$

denote the  $\alpha$ -quantile of the  $B$  centered bootstrap statistics  $\hat{g}^*(\tau) - \tilde{g}(\tau)$ . These bootstrap quantiles are used to construct confidence bands as described below.

Note that in Step 1 of the above algorithm, a different bandwidth is used to perform the non-parametric estimation. We suggest to use the larger bandwidth  $\tilde{h} = 0.5h^{5/9}$ . This produces an

oversmoothed estimate as starting point for the bootstrap procedure. Details on this issue as well as the asymptotic validity of the bootstrap method are shown in Friedrich et al. (2019).

Using Algorithm 3, we can obtain pointwise bootstrap confidence intervals for the nonparametric trend  $g(\tau)$  with a confidence level of  $(1 - \alpha)$ . They are denoted by  $I_{T,\alpha}^{(p)}(\tau)$  and are constructed such that

$$\liminf_{T \rightarrow \infty} \mathbb{P} \left( g(\tau) \in I_{T,\alpha}^{(p)}(\tau) \right) \geq 1 - \alpha \quad \tau \in (0, 1). \quad (4.5)$$

Using the  $\alpha$ -quantiles from Step 5 of the bootstrap algorithm, we can generate such pointwise intervals as

$$I_{T,\alpha}^{(p)}(\tau) = \left[ \hat{g}(\tau) - \hat{q}_{1-\alpha/2}, \hat{g}(\tau) - \hat{q}_{\alpha/2} \right]. \quad (4.6)$$

These intervals are constructed separately for each point  $\tau$ . Therefore, a link over time cannot be established with these intervals. Many interesting research questions, like whether a coefficient remains zero over the whole period or whether there was an upward trend over a certain period of time, cannot be answered with pointwise confidence intervals. The concept of simultaneous confidence bands can be used to answer these questions. In the same notation, the following asymptotic bands are simultaneous over the whole sample

$$\liminf_{T \rightarrow \infty} [\mathbb{P} (g(\tau) \in I_\alpha(\tau) \quad \tau \in (0, 1))] = 1 - \alpha. \quad (4.7)$$

Practical implementation follows a three-step procedure which was first presented in this context by Bühlmann (1998). It is a search algorithm based on the ordered deviations,  $\hat{g}^*(\tau) - \tilde{g}(\tau)$ , of bootstrapped estimates from the original estimate. The first step is to construct pointwise quantiles in the same way as described in Step 5 of Algorithm 2. Formally, the three steps are:

**Algorithm 4** (Simultaneous confidence bands).

1. For all  $\tau \in (0, 1)$ , obtain pointwise quantiles, varying  $\alpha_p \in [1/B, \alpha] : \hat{q}_{\alpha_p/2}(\tau), \hat{q}_{1-\alpha_p/2}(\tau)$ .
2. Choose  $\alpha_s$  as

$$\alpha_s = \operatorname{argmin}_{\alpha_p \in [1/B, \alpha]} \left| \mathbb{P}^* \left[ \hat{q}_{\alpha_p/2}(\tau) \leq \hat{g}^*(\tau) - \tilde{g}(\tau) \leq \hat{q}_{1-\alpha_p/2}(\tau) \quad \forall \tau \in (0, 1) \right] - (1 - \alpha) \right|$$

3. Construct the simultaneous confidence bands as

$$I_{\alpha_s}(\tau) = \left[ \hat{g}(\tau) - \hat{q}_{1-\alpha_s/2}(\tau), \hat{g}(\tau) - \hat{q}_{\alpha_s/2}(\tau) \right] \quad \tau \in (0, 1).$$

In the second step of this procedure, a pointwise error  $\alpha_s$  is found for which a fraction of approximately  $(1 - \alpha)$  of all centered bootstrap estimates falls completely within the resulting confidence intervals. This value  $\alpha_s$  is then fixed and the resulting pointwise confidence intervals with coverage  $(1 - \alpha_s)$  become simultaneous confidence bands with coverage  $(1 - \alpha)$ .

### 4.1.3 Data application

We now apply this procedure. In order to estimate the trend function, we first calculate the residuals from a regression of the ethane data on three Fourier terms. From the residuals we estimate the trend function nonparametrically using the local constant kernel estimator with the Epanechnikov kernel. Bandwidth selection using the Modified Cross Validation (MCV) approach of Chu and Marron (1991) with  $k = 5$  gives a bandwidth of  $h = 0.03$ .

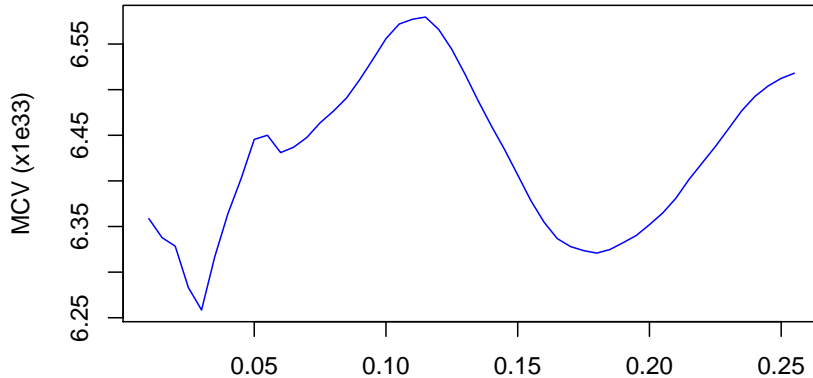


Figure 2: Modified Cross Validation Criterion for a range of bandwidths)

As bandwidth selection is an important part of this procedure, we would like to highlight that the MCV procedure has to be applied with care. The range of possible bandwidths over which we minimize the criterion can have a major effect on the resulting optimal bandwidth. The criterion function can have multiple local minima or, if the values contained in our range are too small, the function can be monotonically increasing such that we always select the smallest possible bandwidth. We allow for values between 0.01 and 0.25 in steps of 0.005. This yields a total of 49 possible bandwidths. To illustrate, we plot the criterion as a function of the bandwidth in Figure 2. We can see a global minimum at 0.03 which is the bandwidth we select. A second (local) minimum can be observed at 0.065 and a third minimum lies at 0.185. Table 3 in the Appendix gives an overview of bandwidth selection performed for the other series. In case of the Jungfrauoch data, we decide to select the global minimum, since the resulting trend curve gives a reasonably smooth estimate which allows us to detect interesting features of the trend. Note that the main conclusions we draw below hold with both candidate bandwidths.

Figure 3 plots the seasonally adjusted data points and the nonparametric trend with the 95% simultaneous confidence bands. If we follow the movements of the trend curve, we see local peaks around the years of 1998 and 2002-2003, which were not visible in the previous analysis. The capture of these two events is possible thanks to the flexibility of the nonparametric approach, since it does not impose the trend to consist of two linear trend lines which is crucial in the parametric procedure. The peaks can be attributed to boreal forest fires which were taking place mainly in Russia during both periods. Geophysical studies have investigated these events in association with anomalies in carbon monoxide emissions (Yurganov et al., 2004, 2005). In such fires, carbon monoxide is co-emitted with ethane, such that these events are likely explanations for the peaks we observe.

We nevertheless observe a significant upward trend towards the end of the sample period as in the parametric analysis. Looking at the confidence bands over the last period - starting in 2009 - it is impossible to completely embed a horizontal line into the bands, signaling strong evidence of a nonzero upward trend. In Friedrich et al. (2019), it is additionally shown that all seasonal effects are captured by the model using three Fourier terms. Results for the other series are plotted in Figure 5 with a repetition of Figure 3 in the top left panel for completeness.

## 4.2 Inference on trend shapes

Based on the trend estimates from previous sections, we are interested in particular features of the trend curve. Having in mind the shape of the trends that we discovered, one important feature for our analysis is the local minimum around 2007/2008 of the trend in the Jungfraujoch ethane column series. Some other ethane series also display a (local) minimum sometime around the period 2008-2010. Therefore, we are interested in the uncertainty around the location of this minimum. In order to investigate this issue, we propose to use the bootstrap method presented above with an additional step to construct confidence intervals around the minimum location. This is discussed in the first part of this section. The analysis can equally be applied to a local maximum of the trend curve, it is not restricted to the analysis of local minima.

Another interesting feature is the resulting post-minimum upward trend. We have a closer look at the specific form of this trend in the second part. Specifically, we suggest two formal tests; one will compare the nonparametric trend to a linear trend and the other one tests for monotonic behavior in the nonparametric trend. All approaches are applied to investigate the trend in the Jungfraujoch series in the final part of this section.

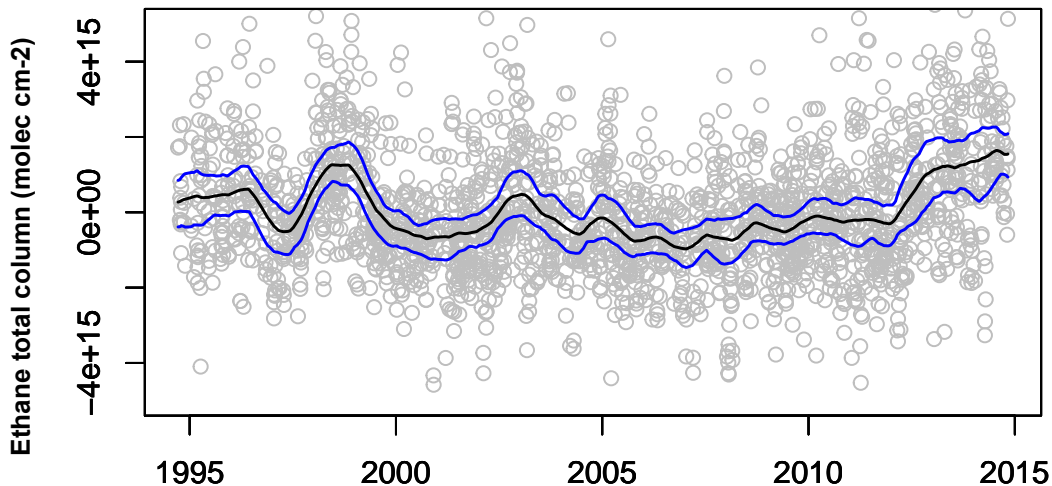


Figure 3: Nonparametric trend estimate and confidence bands ( $h = 0.03$ )

### 4.2.1 Analyzing the locations of extrema

The bootstrap method we use is a simple modification of the bootstrap presented in Section 4. Now we are interested in its minimum which we denote by  $\hat{g}_{min}$  and its location by  $t_{min}$ . Our goal is to construct a confidence interval for  $t_{min}$ . For this new application, we follow Steps 1-3 of the bootstrap algorithm as before to obtain the bootstrap observations to which we apply the nonparametric estimator. This is the same approach as above, the only new step is that we now determine the location of the local minimum for each bootstrap trend closest to  $t_{min}$  – the original minimum – and denote it by  $t_{min}^*$ . To be more specific, look at the following bootstrap algorithm:

**Algorithm 5** (Autoregressive Wild Bootstrap - Minimum location).

1. Repeat steps 1 to 4 of Algorithm 3.
2. Determine all local minima of  $\hat{g}^*(t/T)$ ,  $t = 1, \dots, T$ , and select the one closest to  $t_{min}$ . Denote the selected position by  $t_{min}^*$ .
3. Repeat Steps 1 and 2  $B$  times to obtain the empirical distribution of  $t_{min}^*$ .

In the above algorithm, we need to ensure that we identify the minimum in the bootstrap trend which corresponds to the original global minimum  $t_{min}$ . This does not necessarily have to be the global minimum of the bootstrap trend, which could lie far away from the original global minimum. As an empirically satisfactory solution, we therefore use the closest local minimum in Step 2.

The proposed analysis can be used to obtain further evidence on the location of a potential trend reversal and the results could be compared to the break location found in the linear trend analysis discussed in Section 3. Compared to the previous analysis, the new approach is less robust in a sense that it is sensitive to the choice of bandwidth that was used to generate the nonparametric trend estimate. It is, however, much more flexible and less restrictive than the breakpoint detection, as we do not force the trend before and after the minimum to be linear. We will apply this new approach to the ethane data in Section 4.2.4.

### 4.2.2 A bootstrap-based test for linearity

When comparing both approaches, the (piecewise) linear and the nonlinear, an obvious question arises as to whether we can say more about the appropriateness of the two trend shapes. While the linear trend has some desirable properties – e.g. we get an estimate of the average annual decrease or increase in the data – it might be too restrictive to model the underlying true trend. Kapetanios (2008) designs a bootstrap-based test which can be used to test for parameter constancy under the null hypothesis against smoothly occurring structural change under the alternative. Based on this work, we propose a modification of the test which is able to provide evidence if a certain parametric shape is appropriate to describe the trend in the data at hand. If the true trend follows a certain parametric shape, using an adequate estimator (e.g. the ordinary least squares (OLS) estimator in the linear trend case) is desirable.

For our ethane application, of special interest would be linearity under the null hypothesis. We start by introducing the test in a general framework. The more specific case of linearity will be



discussed later. For the general framework, consider the following null hypothesis:

$$H_0 : g(t) = g_0(\boldsymbol{\theta}, t) \quad \forall t \in \mathcal{G}_m,$$

where  $g_0(\boldsymbol{\theta}, \cdot)$  belongs to a parametric family  $\mathbf{G} = \{g(\boldsymbol{\theta}, \cdot); \boldsymbol{\theta} \in \Theta \subset \mathbb{R}^d\}$  with  $d$  being the number of parameters in  $\boldsymbol{\theta}$ . Further, the set  $\mathcal{G}_m = \{t_1, t_2, \dots, t_m\}$  contains the time points for which the hypothesis should be tested. Under the alternative, the trend does not follow the parametric shape given by  $g_0(\tau)$ , but can be expressed as in model (4.1). As a special case of the test we can for example consider the linear trend function  $g_0(t) = \alpha + \beta t$  such that  $\boldsymbol{\theta} = (\alpha, \beta)$  and  $d = 2$ . As test statistic in the general case, we use an adaption of the test statistic  $\mathcal{T}^{\tau, (\ell)}$  in Kapetanios (2008).

$$Q^t = \left( \hat{g}(t/T) - g_0(\hat{\boldsymbol{\theta}}, t) \right)^2, \quad (4.8)$$

where  $\hat{g}(t/T)$  denotes the nonparametric kernel estimator, as before, and  $\hat{\boldsymbol{\theta}}$  denotes the parameter estimates under the null hypothesis. The type of estimator we choose under the null hypothesis depends on the specific case and the form of the parametric function. In the linear trend case, we can use OLS to obtain estimates  $\hat{\alpha}$  and  $\hat{\beta}$ .

As the superscript  $t$  shows, this test statistic is pointwise. Since we are interested in the trend over time, we follow Kapetanios (2008) and use the three summary statistics for the set  $\mathcal{G}_m = \{t_1, t_2, \dots, t_m\}$  listed below:

$$Q_{ave} = \frac{1}{m} \sum_{j=1}^m \mathcal{T}^{t_j} \quad (4.9)$$

$$Q_{sup} = \sup_j \mathcal{T}^{t_j} \quad (4.10)$$

$$Q_{exp} = \frac{1}{m} \sum_{j=1}^m e^{\frac{\mathcal{T}^{t_j}}{2}} \quad (4.11)$$

To obtain critical values for the test statistics, we rely again on the same bootstrap method. As Kapetanios (2008) stresses that asymptotic tests show a particularly poor performance in his setting and therefore, we assume that a bootstrap-based test is also preferred in our slightly different scenario. The bootstrap algorithm is presented next.

**Algorithm 6** (Autoregressive Wild Bootstrap - Test for a specific trend shape).

1. Estimate  $\hat{g}(t/T)$  as in (4.2) for  $t = 1, \dots, T$ . Obtain the estimate  $\hat{\boldsymbol{\theta}}$  using all data points  $t \in \mathcal{G}_m$ . Then define  $\tilde{g}(t)$  as

$$\tilde{g}(t) \equiv \begin{cases} g_0(\hat{\boldsymbol{\theta}}, t) & \text{for } t \in \mathcal{G}_m, \\ \hat{g}(t/T) & \text{otherwise.} \end{cases}$$

Obtain a combined residual series  $\hat{\epsilon}_t = M_t(\hat{u}_t - \tilde{g}(t))$  for  $t = 1, \dots, T$ .

2. For  $0 < \gamma < 1$ , generate  $\nu_1^*, \dots, \nu_n^*$  as i.i.d.  $\mathcal{N}(0, 1 - \gamma^2)$  and let  $\xi_t^* = \gamma \xi_{t-1}^* + \nu_t^*$  for  $t = 2, \dots, T$ . Take  $\xi_1^* \sim \mathcal{N}(0, 1)$  to ensure stationarity of  $\{\xi_t^*\}$ .

3. Calculate the bootstrap errors  $\epsilon_t^*$  as  $\epsilon_t^* = M_t \xi_t^* \hat{\epsilon}_t$  and generate the bootstrap observations  $\{\hat{u}_t^*\}_{t=1}^T$  by adding the bootstrap errors to the corresponding trend estimate obtained in Step 1:

$$\hat{u}_t^* = M_t (\tilde{g}(t) + \epsilon_t^*).$$

4. Construct bootstrap versions of the pointwise and summary test statistics and denote them by  $Q^{t*}$  and  $Q_i^*$  with  $i = \text{ave}, \text{sup}, \text{exp}$  for  $t \in \mathcal{G}_m$ .
5. Repeat Steps 2 to 4 of this algorithm  $B$  times to obtain the empirical distribution of  $Q_i^*$  with  $i = \text{ave}, \text{sup}, \text{exp}$  and calculate the corresponding critical values and  $p$ -values from it.

The exact specification of the set  $\mathcal{G}_m$  highly depends on the application at hand. In practice, often a set of several consecutive points is needed to be able to estimate the parameters under the null hypothesis. This is the case, for example, with the linear trend application that we focus on in the remainder of the section.

### 4.2.3 Two tests for monotonicity

In the previous section we proposed a bootstrap-based test to investigate if the trend can be best described by a specific parametric shape – in this case linearity – or by the unrestricted nonparametric alternative. In some applications, however, it might not be the most pressing question if the trend follows a specific form. The question whether the trend has been monotonically increasing or decreasing over a certain period can already be enough evidence. In the case of the ethane series, geophysicists are mainly interested in establishing an upward trend in the post-minimum period of the sample. Therefore, we propose to additionally use two tests for monotonicity.

For these tests, we consider a situation where the trend function is monotonically increasing under the null hypothesis. The alternative is the same as before, a nonparametric unrestricted trend. Formally, this can be written as:

$$H_0 : m(\cdot) \text{ is an increasing function on } \mathcal{I},$$

or, since under the given smoothness assumptions the function  $m(\cdot)$  is differentiable:

$$H_0 : m'(t/T) \geq 0 \quad \forall t \in \mathcal{I}.$$

In this case, the set  $\mathcal{I}$  must be a compact interval in the domain of the function  $m(\cdot)$ . The paper by Ghosal et al. (2000) proposes the following test statistic to test the above null hypothesis, for  $t \in \mathcal{I}$ :

$$U_1^t = -\frac{2}{T(T-1)} \sum_{1 \leq i < j \leq T} \text{sign}(y_j - y_i) \frac{1}{h_U} K\left(\frac{i/n - t/n}{h_U}\right) \frac{1}{h_U} K\left(\frac{j/n - t/n}{h_U}\right) \quad (4.12)$$

with

$$\text{sign}(x) = \begin{cases} 1 & \text{if } x > 0 \\ 0 & \text{if } x = 0 \\ -1 & \text{if } x < 0 \end{cases}$$

As kernel function, we use  $K(x) = 0.75(1 - x^2)$  for  $-1 < x < 1$  and 0 otherwise, as Ghosal et al. (2000) suggests. We also follow their bandwidth recommendation  $h_U = 0.5T^{-1/5}$ . The test is based on the idea that for an increasing function, increments will be positive and thus, the test statistic should satisfy  $U_1^t \leq 0$  for most  $t \in \mathcal{I}$  under the null. This can be easily verified as  $U_1^t$  sums over weighted differences of observations  $(y_j - y_i)$  such that  $j > i$ ; or more precisely, it sums over the sign thereof. The test statistic  $U_1^t$  corresponds to one point in the interval of interest,  $\mathcal{I}$ , similar to the test statistic  $Q^t$  in (4.8). As summary statistic, Ghosal et al. (2000) propose a supremum statistic

$$U_{1,sup} = \sup_{t \in \mathcal{I}} U_1^t. \quad (4.13)$$

Additionally, we use a second test to support our findings. This test is proposed in Chetverikov (forthcoming). The difference compared to (4.12) is the use of the sign function, which is omitted in this version of the test. The full differences and not only their sign will be accounted for. This gives the following test statistic:

$$U_2^t = -\frac{2}{T(T-1)} \sum_{1 \leq i < j \leq T} (y_j - y_i) \frac{1}{h_U} K\left(\frac{i/n - t/n}{h_U}\right) \frac{1}{h_U} K\left(\frac{j/n - t/n}{h_U}\right), \quad (4.14)$$

which we apply with the same specifications as we use for  $U_1^t$ . Again, this statistic should be negative under the null hypothesis due to the same reason as above. In line with the above procedure, we calculate summary test statistics  $U_{2,sup}$  whose exact definition follow in analogy to  $U_{1,sup}$ .

To obtain critical values, we rely once again on the autoregressive wild bootstrap. In this case, we do not need to make many adjustments to the standard bootstrap algorithm in Section 4.1.2 for the creation of confidence intervals. Once the bootstrap observations are generated in Step 3, we calculate the test statistics (4.12) and (4.14). Subsequently, we obtain the bootstrap version  $U_1^{t,*}$  and  $U_2^{t,*}$  as well as the summary versions. For the linearity testing in the previous section, we needed to estimate a linear trend for part of the sample to be able to conduct the test and thus, an adaption of the bootstrap algorithm was needed, which is not the case here.

#### 4.2.4 Data application

We now demonstrate the usefulness of our proposed tests by applying it to the Jungfraujoch data. The minimum of interest of the nonparametric trend as seen in Figure 3 is located at 2007.04. When applying the bootstrap tool to obtain 95% confidence intervals, we find them to range from 2006.30 to 2007.68, which is located slightly earlier than the confidence interval of the break location in the parametric setting (2008.35 to 2010.03). Although both results are constructed using substan-

tially different approaches, the intervals lie close together. The nonparametric approach results in a smooth trend, while the parametric specification includes an abrupt break through which the minimum is defined. Similar results can be obtained for the Toronto ethane series with a minimum in 2008.84 and the 95% confidence interval ranging from 2007.30 to 2010.36. Of special interest in our ethane series analysis is the post minimum development of the trend. Multiple series in the Northern Hemisphere display an upward trend after 2007/2008 and in previous research this trend has been modeled by a linear trend. Our approach goes back one step and first investigates the question whether a linear trend or a non-linear trend as in the nonparametric case is preferred. To this end, we apply the above procedure with a linear trend specification under the null to the Jungfraujoch data. For this we select the set  $\mathcal{G}_m$  in such a way that it covers the period after 2007.04 where the minimum is obtained.

As mentioned above, in the case of a linear trend under the null hypothesis, we need the set to consist of a series of consecutive points to be able to estimate the slope parameter. This is done here by taking approximately the last quarter of the sample. If it was exactly the last quarter, the set would look like  $\mathcal{G}_m = \left\{ \frac{3}{4}T, \frac{3}{4}T + 1, \dots, T \right\}$ , which satisfies the theoretical requirements. Under the null, the trend curve is designed in such a way that the linear trend starts at the point where the nonparametric trend ends. Thus, it starts at the point  $\hat{g}_{min}$ . Therefore, the intercept is fixed and only the slope parameter is estimated under the null hypothesis by OLS. For the calculation of the test statistic (4.8) we use as  $g_0(\hat{\theta}, t)$  the best fitting linear trend line that goes through the minimum for all  $t$  in  $\mathcal{G}_m$ .

An application of this procedure to the Jungfraujoch ethane series gives us three  $p$ -values of  $p_{ave} = 0.002$ ,  $p_{sup} = 0.004$  and  $p_{exp} = 0.000$ . We note that for the exponential summary statistic to work, we first need to downscale the series by  $10^{13}$ . This does not change the shape of the trend, it just makes the test feasible. All three tests unanimously reject the null hypothesis of a linear trend for the last period of the sample.

Coming back to the original research question and motivation for this test, we now investigate the post-minimum nonparametric trend of the Jungfraujoch ethane series. After having rejected linearity, this test helps us to establish whether there has been a monotonic upward trend in the series since the minimum at the beginning of 2007. This defines the way we choose the interval  $\mathcal{I}$  in this application over which we test for monotonicity - the starting point is the minimum at 2007.04 and the end point is the end of the sample at 2014.83. The interval thus defined contains 930 out of the 2260 time points. It coincides with the set of points we chose for the linearity test above.

After computing the two different versions  $U_1^t$  and  $U_2^t$  with  $h_U = 0.107$  for all points in the interval, we obtain  $U_{1,sup} = -0.008$  and  $U_{2,sup} = -4.061 \times 10^{13}$ . The bootstrap critical values for the tests are 0.0269 and  $1.176 \times 10^{14}$ , respectively, which yield  $p$ -values of 0.371 for  $U_{1,sup}$  and 0.863 for  $U_{2,sup}$ . Therefore, we cannot reject the null hypothesis and conclude that the post-minimum trend in the ethane burden on top of the Jungfraujoch is likely to be monotonically increasing.

## 5 Conclusion

In this paper, two approaches are proposed to estimate trends in climate time series: a broken linear trend model with unknown break date and a nonlinear trend model, which is estimated nonparametrically. Both methods are applied to a time series of ethane total columns measured at a station in the Swiss Alps. The high-altitude station located at the Jungfraujoeh records daily observations of ethane abundance in the atmosphere. Depending on the conditions, however, measurements cannot be made every day resulting in a daily time series with approximately 70% missing observations. This is a limitation frequently encountered in (climatological) time series. It causes a problem when we want to construct confidence intervals around the trend estimate. An additional complication arises due to strong seasonal effects, which cause the residuals from both models to be serially correlated. In order to resolve these issues, we suggest an autoregressive wild bootstrap method for the construction of confidence intervals around the break location and the parameter estimates of the parametric model. For the nonparametric model, we propose a battery of diagnostic tools to investigate the shape of the resulting trend.

Results from this application indicate that there is a significant upward trend in atmospheric ethane, starting around 2007/2008. This is confirmed by both approaches, the break of the linear model is located at the beginning of 2009, while the local minimum of the nonparametric approach is in 2007. Additionally, after 2007 we cannot embed a straight line into the simultaneous confidence bands around the nonparametric trend estimate which is supported by the subsequent results of a formal test for linearity. All three proposed test statistics indicate that a linear trend is not appropriate for the post-minimum period of the Jungfraujoeh data. In addition, the nonparametric estimation reveals a trend function which exhibits a local maximum around the years of 1998 and 2002-2003 which coincide with boreal forest fires in Russia.

Given both sets of results, it should be stressed that the two approaches proposed in this chapter can be seen as complimentary rather than competing methods. The simplicity of the broken linear trend model allows us to indicate a numerical value for the slope parameter, summarizing the development of the trend over a particular period. The complexity of the nonlinear approach has the potential of providing us with additional information, while at the same time it can be used to confirm previous findings.

One, perhaps seemingly unnecessary, limitation of the broken linear trend model, is that it can accommodate only one break, putting it at a natural disadvantage to the more flexible nonparametric approach. Indeed, estimation of broken linear trend models with multiple breaks at unknown locations can be estimated using, for instance, the methods proposed in Bai and Perron (1998), which also allow one to test for the number of breaks in the trend. Constructing confidence intervals for the locations of the breaks is, however, more complicated in such models. It can be a powerful tool for the analysis of more complicated time series than atmospheric ethane, whose properties are less well studied. The extension of the bootstrap methodology to multiple breaks is left for future research.

## Acknowledgments

The FTIR data used in our Appendix were obtained from J.W. Hannigan (National Center for Atmospheric Research, Boulder, CO), K. Strong (University of Toronto, Toronto, ON) and D. Smale (National Institute of Water and Atmospheric research, Lauder, NZ), mostly as part of the Network for the Detection of Atmospheric Composition Change (NDACC). NDACC data are publicly available at <http://www.ndacc.org>. We gratefully acknowledge their respective contributions. The NIWA FTIR program is funded through the New Zealand government's core research grant framework from the Ministry of Business, Innovation and Employment.

## References

- Bai, J. and P. Perron (1998). Estimating and testing linear models with multiple structural changes. *Econometrica* 66(1), 47-78.
- Bühlmann, P. (1998). Sieve bootstrap for smoothing in nonstationary time series. *Annals of Statistics* 26, 48-83.
- Chetverikov, D. (forthcoming). Testing regression monotonicity in econometric models. *Econometric Theory*, 1-48. doi:10.1017/S0266466618000282
- Chu, C.-K. and J.S. Marron (1991). Comparison of two bandwidths selectors with dependent errors. *The Annals of Statistics* 19(4), 1906-1918.
- De Smedt, I., Stavrakou, T., Müller, J.-F., van der A, R.J. and M. Van Rosendael (2010). Trend detection in satellite observations of formaldehyde tropospheric columns. *Geophysical Research Letters* 37, L18808.
- Franco, B., Bader W., Toon G.C., Bray C., Perrin A., Fischer E.V., Sudo K., Boone C.D., Bovya B., Lejeune B., Servais C. and E. Mahieu (2015). Retrieval of ethane from ground-based FTIR solar spectra using improved spectroscopy: Recent burden increase above Jungfraujoch. *Journal of Quantitative Spectroscopy and Radiative Transfer* 160, 36-49.
- Franco, B., Mahieu, E., Emmons, L.K., Tzompa-Sosa, Z.A., Fischer, E.V., Sudo, K., Bovy, B., Conway, S., Griffin, D., Hannigan, J.W., Strong, K. and K.A. Walker (forthcoming). Evaluating ethane and methane emissions associated with the development of oil and natural gas extraction in North America. *Environmental Research Letters*, 11(4), 044010, doi:10.1088/1748-9326/11/4/044010, 2016.
- Friedrich, M., Smeekes, S. and J.-P. Urbain (2019). Autoregressive wild bootstrap inference for nonparametric trends. *Journal of Econometrics - Annals issue on econometric models of climate change*, forthcoming.
- Gardiner, T., Forbes, A. , de Mazière, M., Vigouroux, C., Mahieu, E., Demoulin, P., Velasco, V., Notholt, J., Blumenstock, T., Hase, F., Kramer, I., Sussmann, R., Stremme, W., Mellqvist, J., Strandberg, A., Ellingsen, K. and M. Gauss (2008). Trend analysis of greenhouse gases over Europe measured by a network of ground-based remote FTIR instruments. *Atmospheric Chemistry and Physics* 8, 6719-6727.
- Ghosal, S., Sen, A. and A. van der Vaart (2000). Testing Monotonicity of Regression, *The Annals of Statistics* 28, 1054-1082.
- Hausmann, P., Sussmann, R. and D. Smale (2016). Contribution of oil and natural gas production to renewed increase in atmospheric methane (2007-2014): top-down estimate from ethane and methane column observations. *Atmos. Chem. Phys.*, 16, 3227-3244.

- Helmig, D., Rossabi, S., Hueber, J., Tans, P., Montzka, S.A., Masarie, K., Thoning, K., Plass-Duelmer, C., Claude, A., Carpenter, L.J., Lewis, A.C., Punjabi, S., Reimann, S., Vollmer, M.K., Steinbrecher, R., Hannigan, J.W., Emmons, L.K., Mahieu, E., Franco, B., Smale, D. and A. Pozzer (2016). Reversal of global atmospheric ethane and propane trends largely due to US oil and natural gas production. *Nature Geoscience* 9, 490-495.
- Kapetanios, G. (2008). Bootstrap-based tests for deterministic time-varying coefficients in regression models. *Computational Statistics and Data Analysis* 53, 534-545.
- Mahieu, E., Chipperfield, M.P., Notholt, J., Reddman, T., Anderson, J., Bernath, P.F., Blumenstock, T., Coffey, M.T., Dhomse, S.S., Feng, W., Franco, B., Froidevaux, L., Griffith, D.W.T., Hannigan, J.W., Palm, M., Paton-Walsh, C., Russell III, J.M., Schneider, M., Servais, C., Smale, D. and K.A. Walker (2014). Recent Northern Hemisphere stratospheric HCl increase due to atmospheric circulation changes. *Nature* 515, 104-107.
- Neumann, M.H. and J. Polzehl (1998). Simultaneous bootstrap confidence bands in nonparametric regression. *Journal of Nonparametric Statistics* 9, 307-333.
- Vinciguerra, T., Yao, S., Dadzie, J., Chittams, A., Deskins, T., Ehrman, S. and R.R. Dickerson (2015). Regional air quality impacts of hydraulic fracturing and shale natural gas activity: evidence from ambient VOC observations. *Atmos. Environ.* 110, 144-50.
- Yurganov, L.N., Blumenstock, T., Grechko, E.I., Hase, F., Hyer, E.J., Kasischke, I.S., Koike, M., Kondo, Y., Kramer, I., Leung, F.-Y., Mahieu, E., Mellqvist, J., Notholt, J., Novelli, P.C., Rinsland, C.P., Scheel, H.E., Schulz, A., Strandberg, A., Sussmann, R., Tanimoto, H., Velazco, V., Zander, R. and Y. Zhao (2004). A quantitative assessment of the 1998 carbon monoxide emission anomaly in the Northern Hemisphere based on total column and surface concentration measurements. *Journal of Geophysical Research* 109, D15305.
- Yurganov, L. N., Duchatelet, P., Dzhola, A. V., Edwards, D. P., Hase, F., Kramer, I., Mahieu, E., Mellqvist, J., Notholt, J., Novelli, P.C., Rockmann, A., Scheel, H.E., Schneider, M., Schulz, A., Strandberg, A., Sussmann, R., Tanimoto, H., Velazco, V., Drummond, J.R. and J.C. Gille (2005). Increased Northern Hemispheric carbon monoxide burden in the troposphere in 2002 and 2003 detected from the ground and from space. *Atmospheric Chemistry and Physics*, 5(2), 563-573.
- Zeng, G., Wood, S.W., Morgenstern, O., Jones, N.B., Robinson, J. and D. Smale (2012), Trends and variations in CO, C<sub>2</sub>H<sub>6</sub>, and HCN in the Southern Hemisphere point to the declining anthropogenic emissions of CO and C<sub>2</sub>H<sub>6</sub>. *Atmospheric Chemistry and Physics*, 12(16), 7543-7555.

## Appendix A Additional results

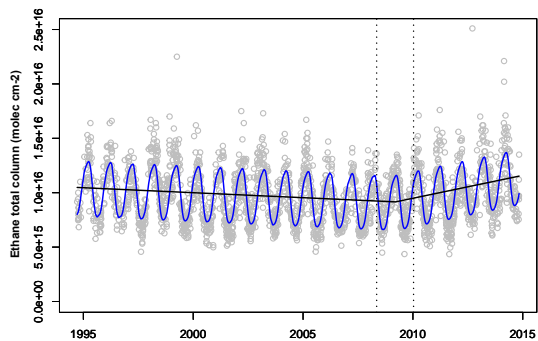
In this first part of the Appendix we give additional results for the complete set of ethane series. Table 3 shows results of bandwidth selection for the nonparametric part of the analysis. They are obtained by setting  $k = 5$  in 4.3, meaning 11 observations are left out in total. Using  $k = 4$



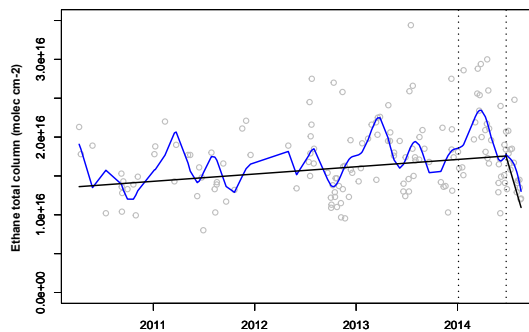
produced almost identical results. Figures 4 and 5 display the results of the broken linear trend and the nonparametric trend, respectively. The latter figure is produced using the first column of bandwidths in Table 3.

	First	Second
Jungfrauoch	0.030	0.065
Boulder	0.060	0.220
Eureka	0.080	0.080
Lauder	0.110	0.220
Thule	0.060	0.120
Toronto	0.085	0.130

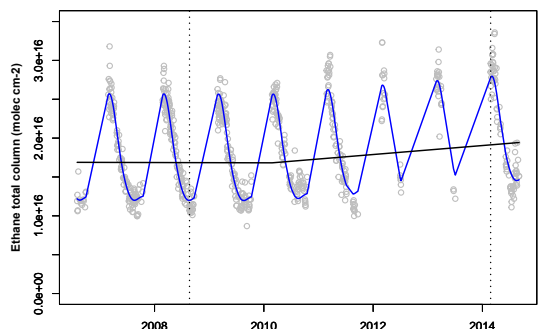
Table 3: Bandwidth selection using MCV with  $k = 5$



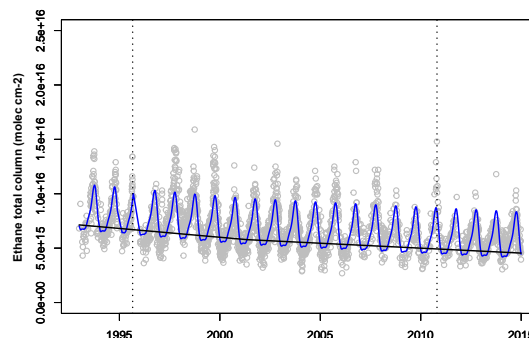
(a) Jungfrauoch



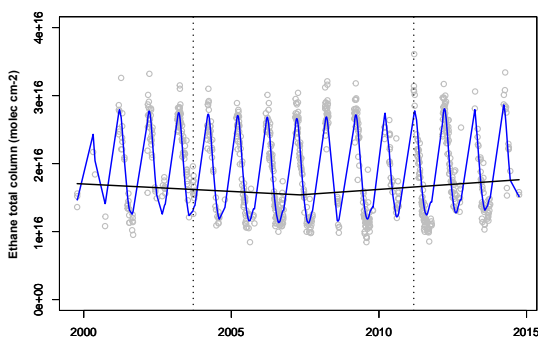
(b) Boulder



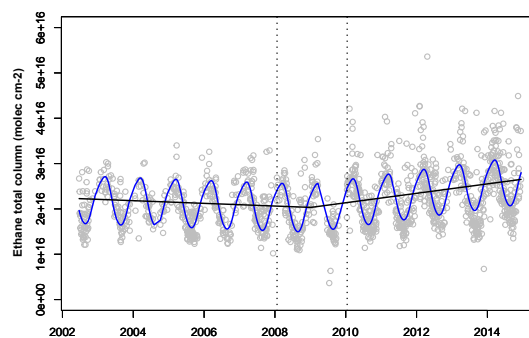
(c) Eureka



(d) Lauder

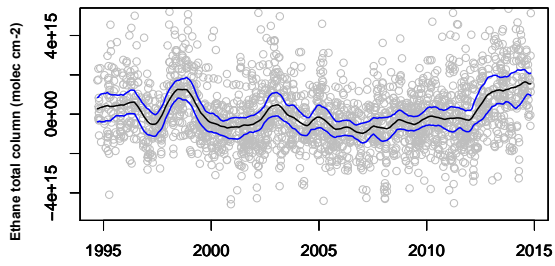


(e) Thule

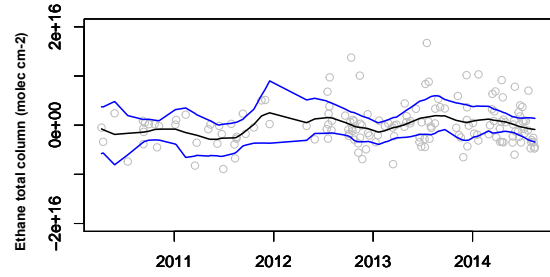


(f) Toronto

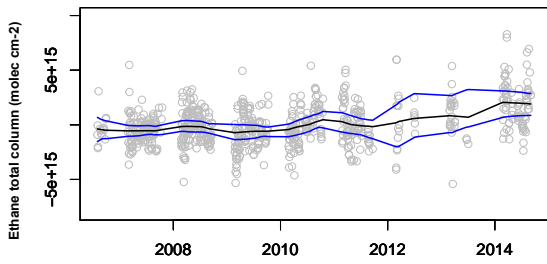
Figure 4: This figure shows the data as well as the continuous broken trend and the fitted Fourier series for all 6 series.



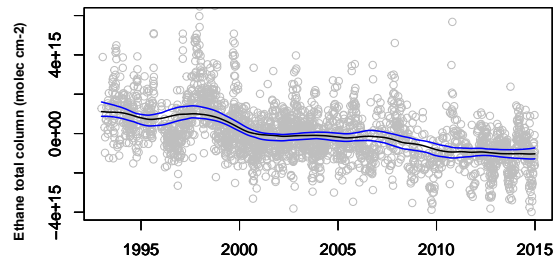
(a) Jungfrauoch



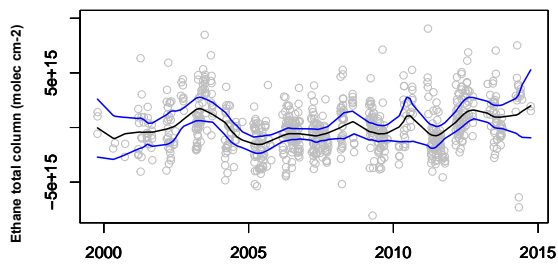
(b) Boulder



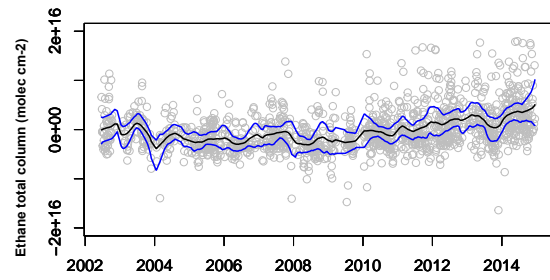
(c) Eureka



(d) Lauder



(e) Thule



(f) Toronto

Figure 5: This figure shows the data, the nonparametric trend functions and the 95% simultaneous confidence bands.